MultiCraft

International Journal of Engineering, Science and Technology
Vol. 2, No. 8, 2010, pp. 118-126

INTERNATIONAL JOURNAL OF ENGINEERING, SCIENCE AND TECHNOLOGY

www.ijest-ng.com

Characterization of γ- and α-Fe_2O_3 nano powders synthesized by emulsion precipitation-calcination route and rheological behaviour of α-Fe_2O_3

S.K. Sahoo [1,*], K. Agarwal [2], A.K. Singh[3], B.G. Polke [1] and K.C. Raha [1]

[1] *High Energy Materials Research Laboratory, Pune-21, INDIA*
[2] *Defence Materials and Stores Research and Development Establishment, Kanpur-208013, INDIA*
[3] *Defence Institute of Advanced Technology, Pune-411025, INDIA*
[*] *Corresponding author: email- saroj_sahu1@rediffmail.com*

Abstract

Nano crystals of γ-Fe_2O_3 (maghemite) were synthesized by emulsion precipitation method using kerosene as oil phase, SPAN-80 (sorbitane monooleate) as the surfactant and sodium hydroxide as the precipitating agent. The characterization of the samples by FTIR (Fourier transform infra-red) and XRD (X-ray diffraction) techniques confirmed the formation of γ-Fe_2O_3 (maghemite). Analysis by SEM (scanning electron microscope) and TEM (transmission electron microscope) was carried out to study the morphology and particle size. The as prepared samples contained inverse spinel cubic phase maghemite. Effect of initial iron concentration on crystallite size of maghemite showed that it decreased with the decrease in initial iron concentration. Transformation of γ-Fe_2O_3 to α-Fe_2O_3 (hematite) was studied by calcining the precursor in the temperature range of 500 to 850°C. Formation/transformation of phases at different temperatures was confirmed by FTIR and XRD studies. Images, obtained by SEM and TEM showed the morphology and nanocrystal formation of hematite. Room temperature rheological behaviour of the synthesized α-Fe_2O_3 nano powder has been studied.

Keywords: Iron oxide, emulsion, nanocrstals, crystal growth, rheological property

1. Introduction

Among the various forms of iron oxides, maghemite (γ-Fe_2O_3) and hematite (α-Fe_2O_3) are of great importance in technological and industrial applications (Huo *et al.*, 2000). Maghemite has numerous applications like recording, memory devices, magnetic resonance imaging, drug delivery or cell targeting (Laurent *et al.*, 2008; Daou *et al.*, 2010). Hematite exhibits high resistance to corrosion, therefore, it has been extensively used in many fields which include photo-anode for photo assisted electrolysis of water. It is an active component of gas sensors, catalyst, lithium ion battery, pigments and oxidizer in thermite composition (Kodama *et al.*, 1997; Fischer and Grubelich, 1998; Dong and Zhu, 2002; Prakash *et al.*, 2004; Gupta and Gupta, 2005; Figuerola *et al.*, 2010). It is also used in magnetic fluids, also called ferrofluids, for damping in inertial motors, shock absorbers, heat transfer fluids, etc (Wang and Meng, 2001; Espı´n *et al.*, 2004). All these engineering applications require study of rheological behavior. Because of extensive applications, nano maghemite and hematite have attracted much attention for their synthesis and applications.

Various methods have been developed to produce maghemite and hematite with controlled shape, size, and size dispersion (Daou *et al.*, 2010). Micronic acicular maghemite was prepared either directly from FeOOH or through a topotatic oxidation of magnetite (Bate, 1975). Maghemite nanoparticles have been obtained by co-precipitation of $FeCl_3$ and $FeCl_2$ in an alkali medium, (Massart, 1981), microemulsion method with ionic surfactants, (Tueros *et al.*, 2003) or physical methods such as high-energy ball-milling (Randrianantoandro *et al.*, 2001). Hematite nanoparticles with different structures have also been synthesized by various methods, such as the sol–gel process (Woo *et al.*, 2003), thermal oxidation of iron metal (Wen *et al.*, 2005), forced hydrolysis (Musi´c *et al.*, 2003), hydrothermal method (Cao *et al.*, 2005; Giria *et al.*, 2005; Baruwati *et al.*, 2006; Jia *et al.*, 2007), gas-phase flame synthesis (Kumfer *et al.*, 2010), ultrasonic spray pyrolysis (Gurmen and Ebin, 2010). Jia *et al.* (2005)) prepared mono-dispersed α-Fe_2O_3 single-crystal nanotubes by a facile hydrothermal method (Jia *et al.,* Chen *et al* (2005) synthesized α-Fe_2O_3 nanotubes by a templating method and studied their gas sensor and lithium-ion battery applications. Gupta and Gupta (2005)

prepared various nano iron oxides for biomedical applications. Vayssieres and co-workers investigated the one-dimensional quantum-confinement effect in α-Fe_2O_3 ultrafine nanorod arrays (Vayssieres *et al.*, 2005). The present study is aimed at synthesizing nano maghemite and hematite using simple and facile emulsion-precipitation followed by calcination method.

The inverse spinel crystal structure is the most general case for maghemite (Pecharroman *et al.*, 1995; Glotch and Rossman, 2009). General formation of hematite is found to be rhombohedrally hexagonal. Phase transformation of α-Fe_2O_3 from other forms of iron oxides, hydroxide and oxy-hydroxides has been reported by many researchers. The formation of $Fe(OH)_3$ by precipitation of Fe^{3+} salt and its transformation to β-FeOOH (akaganeite) and then to α-Fe_2O_3 was proposed by Cao *et al.* (2006). Phase transformation from β-FeOOH to α-FeOOH (goethite) to α-Fe_2O_3 in alkaline medium was reported by Cornel and Schwertmann (1996). It is generally accepted that the phase transformation from β-FeOOH to α-FeOOH and then to α-Fe_2O_3 occurs via the dissolution precipitation mechanism (Music *et al.*, 1997) in aqueous medium. Dar *et al.* (2005) investigated the formation of α-FeOOH to α-Fe_2O_3. Evaluation and investigation of various phases of iron oxides as a function of heat treatment time and temperature has been reported by Deb and Basumallick (2004). Increase in holding time at 250°C caused transformation of Fe_3O_4 (magnetite) to γ- Fe_2O_3 and from γ-Fe_2O_3 to α-Fe_2O_3. Zhao *et al.* (2007) investigated the phase transformation of γ-Fe_2O_3 to α-Fe_2O_3 and found that such a transformation occurred at 770 °C with an exothermic peak in DSC curve. Yen *et al.* (2002) studied the crystallite size variation on formation of α-Fe_2O_3 from γ–FeOOH (lepidocrocite), Fe_3O_4 and amorphous $Fe(OH)_3$ to α-Fe_2O_3. Effect of calcination temperature on crystallite size and crystal growth of iron oxide nano-crystallites was studied by Praserthdam *et al.* (2003).

In view of the importance of nano maghemite and hematite, the present investigations were undertaken to synthesize maghemite nano-crystallites by a facile emulsion method and their transformation to nano-crystals of hematite. Surfactant mediated precursors were prepared at two initial iron concentrations and effect of calcination temperature on phase transformation was followed. The synthesized α-Fe_2O_3 has been used to prepare its colloidal solution (ferrofluid) of different concentrations with a view to study its rheological behavior.

2. Experimental

Anhydrous $FeCl_3$, NaOH, SPAN-80 (all of Analytical grade) and kerosene were used without further purification. 200 mL of $FeCl_3$ solution of 0.5M was taken in a 1000 mL beaker. 2g of SPAN-80 was added with vigorous stirring and the contents were stirred for 15 minutes. 4 mL kerosene was added and stirring was continued for another 30 minutes. The system transformed to turbid emulsion of milky brown colour. NaOH solution (5M) was added drop wise till the pH reached up to 10-10.5. Reddish brown precipitate of iron hydroxide started forming from pH 3 onwards. Precipitate became thick as pH increased. After reaching the desired pH, addition of NaOH was stopped and the stirring was continued for 1h. The contents in the beaker were then left undisturbed for 30 min to allow the precipitate to settle. The precipitate was filtered and washed with distilled water till free of ions and excess alkali. Then it was washed with acetone to remove kerosene and surfactant and kept in an oven at 100 °C overnight. The dried precursor was subjected to calcination at various temperatures i.e. 250, 500 and 850 °C for two hours. After cooling and drying, final product was ground with agate mortar to get fine powder. The sample details and calcination temperature are given in Table 1. Similarly for 0.1M $FeCl_3$ solution (lower concentration), 1M NaOH was used following the same method.

Table 1. Conditions of sample preparation and their coding

Serial No.	Sample	Calcination temp. (°C)	Initial $FeCl_3$ Conc (M)	Surfactant %	Oil %
1	A	100 (oven dried)	0.5	1	2
2	A250	250			
3	A500	500			
4	A850	850			
5	B	100 (oven dried)	0.1	1	2
6	B250	250			
7	B500	500			
8	B850	850			

Infrared spectra of samples were recorded on a Thermonicolet FTIR spectrophotometer (Model Nicolet 5700, make USA) using KBr matrix. XRD patterns were obtained using (Model X'Pert PRO make PANalytical, Netherland) with CuKα source. Particle morphology was studied by obtaining micrographs using Carl Zeiss, EVO50 low vacuum SEM, Germany. TEM and and HRTEM were obtained using FEI make Technai F-30, the Netherland, with 300kV field emission gun,.

Three types of ferrofluids were prepared by dissolving 50 mg, 100 mg and 300 mg each of α-Fe_2O_3 (B850) in 100 ml of ethylene glycol (EG). These solutions were sonicated for 1 h and subsequently 0.5, 1, and 3 ml of acetylacetone (acac) was added and sonicated again for 10 min. The rheological behavior of the suspensions was investigated using Rheologica Nova Rheometer with 40 mm plate-plate geometry at 25 °C temperature.

3. Results and discussion

3.1 FTIR Analysis

Figure1 shows the FTIR spectra of iron oxide samples of series A and sample B850. From the spectra it can be seen that no strong bands were identified for sample A. Two broad peaks at 555 and 463 cm^{-1} were identified for sample A250. These peaks may correspond to Fe-O stretching and bending vibration mode, respectively of γ-Fe_2O_3 (Kim *et al.*, 2010). These two peaks became slightly stronger for sample A500, which may correspond to a partial vacancy ordering in the octahedral positions in the maghemite inverse spinel crystal structure (White and Deangelis, 1967; Faria *et al*, 1997; Millan *et al*, 2007). The characteristic absorption bands of sample A850 at 535 and 462 cm^{-1} and for sample B850 at 538 and 466 cm^{-1} are assigned to Fe-O stretching and bending vibration mode of α-Fe_2O_3 respectively (Zhao *et al.*, 2007).

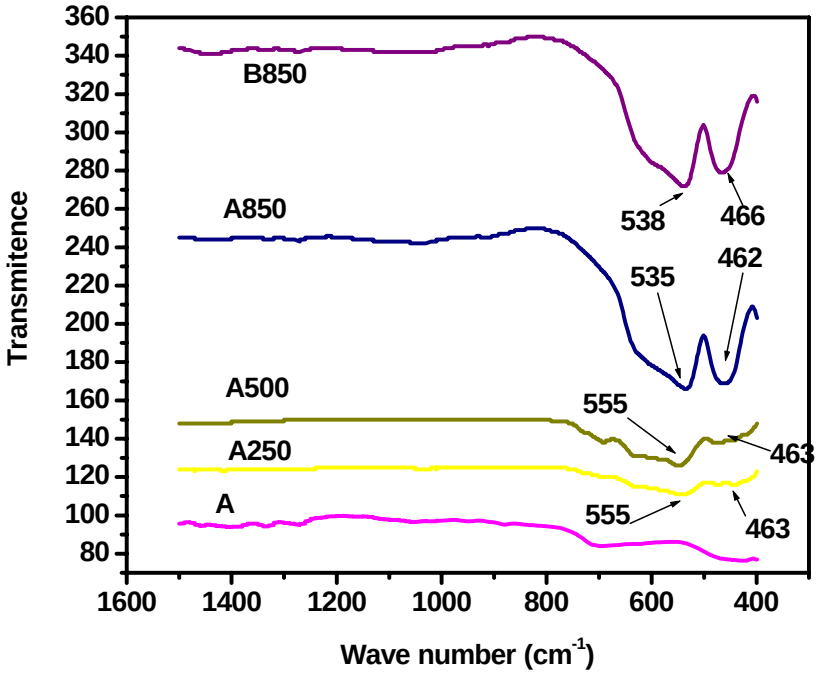

Figure 1. FTIR spectra of iron oxide samples series A and B850.

3.2 XRD analysis

XRD spectra of the A series samples are presented in Figure 2 and those for B series samples are given in Figure 3. The peaks observed at d values of 2.95, 2.51, 2.08, 1.60, 1.47 Å in sample A correspond to cubic phase of maghemite, γ-Fe_2O_3 (matched with PDF No- 01-089-5892).). XRD peaks of sample A250 are almost similar to those of precursor A showing better crystallinity. Sample A500 contains more intense peaks of cubic γ-Fe_2O_3 along with weak α-Fe_2O_3 (peaks marked as 'a'). Sample A850 contains peaks of rhombohedral α-Fe_2O_3 at d-values of 3.62, 2.67, 2.49, 2.19, 1.83, 1.68, 1.59, 1.48, 1.44, 1.30 Å (matched with PDF No-01-079-007). The results show that the crystal formation of hematite phase started at 500 °C. Thus, A500 is the state of both γ-(major) and α-Fe_2O_3 (minor as indicated in figure). γ-Fe_2O_3 particles have cubic unit cells with both octahedrally and tetrahedrally coordinated Fe^{3+} sites (defect spinel structure) whereas the unit cell of α-Fe_2O_3 is hexagonal and contains only octahedrally coordinated Fe^{3+} atoms (corundum structure). Complete phase transformation occurs at 850°C. Crystallographic phases obtained for sample B series are also similar to those of sample A. The difference is that in case of B500, α-Fe_2O_3 peaks were not found. Thus B500 contains peaks of mainly γ-Fe_2O_3. This data helps to synthesize pure γ-Fe_2O_3 for further application and confirms that phase transformation at lower concentration occurs after 500°C.

The values of lattice constants, phase present and crystallite size of various samples are listed in Table 2. Average crystallite size is calculated using broadening of most intense peaks from XRD pattern and Scherrer equation. The line broadening is due to grain surface relaxation of nanocrystalline powders (Scardi, 1999; Leoni *et al.*, 2004; Maensiri *et al.*, 2007). Lattice parameters '*a*' and '*b*' show marginal decrease with increase in calcination temperature from 250 to 500°C but abrupt decrease is observed at 850 °C with the formation of α-Fe_2O_3. Sudden increase in lattice parameter '*c*' is observed with the formation of pure α-Fe_2O_3 phase. In

case of crystallite size of nanoparticles, with increase in calcination temperature, marginal increase in crystallite size was observed upto 500 ^{o}C and with the formation of α-Fe_2O_3 at 850^{o}C, the crystallite size increased from 25.8 to 42.3 nm. Similar results were obtained for B series of samples for lattice parameters.

There is a lot of difference in the particle size of precursor sample A and B with their MCD values as 2.1 and 21.2 nm respectively. It may be explained as follows: an emulsion is composed of two phases, namely water, oil and a mixing agent i.e., surfactant. In oil-in-water emulsion, volume of water phase is more than oil phase. The materials were synthesized with very low concentration of oil and surfactant. Due to vigorous stirring, oil phase is transformed into tiny micro-droplets stabilized by surfactant within the water phase and move very fast. These moving droplets act as collider. At the time of precipitation, the precipitated iron hydroxide is collided by these fast moving oil droplets. Continuous and very fast collision leads to break the hydroxide into nanoparticles. By increasing the number of collisions, smaller particle size may be obtained. As the concentration of iron hydroxide decreases, probability of number of collision per molecule/particle increases and particle size becomes smaller. Thus the precursor sample B is much smaller (2.1nm) when compared to the precursor sample A (21.2nm).

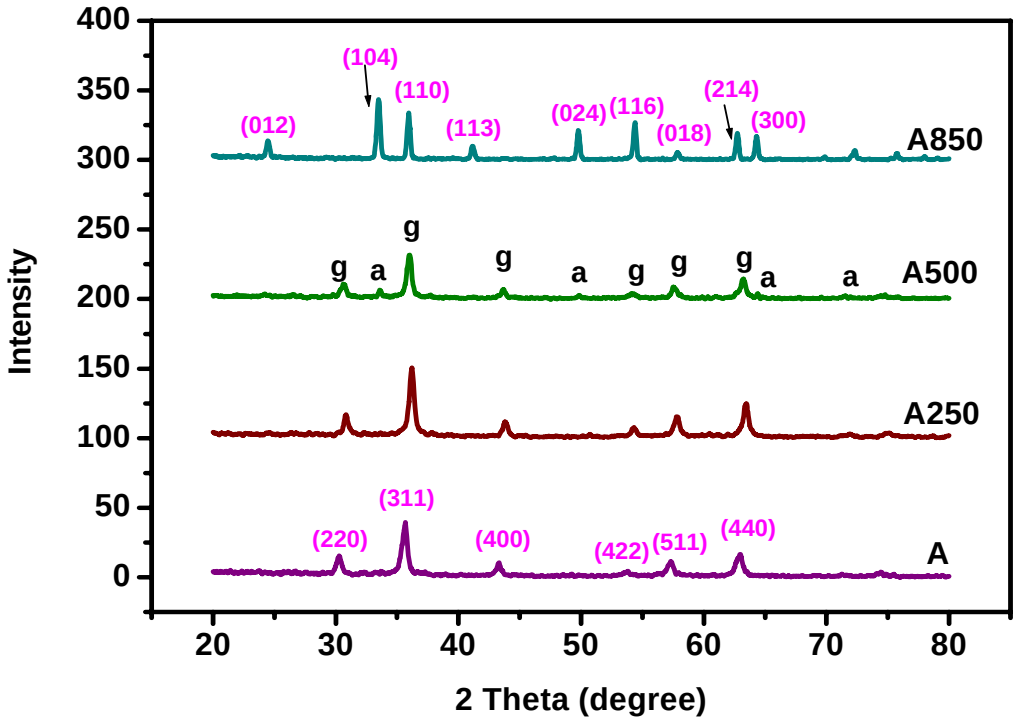

Figure 2. XRD patterns of sample A, A250, A500 and A850. (g : γ-Fe_2O_3 and a : α-Fe_2O_3).

Table 2. Crystallographic data obtained from XRD

Sample	Phases present	Lattice parameters (Å)			d_{XRD} (nm)
		a	*b*	*c*	
A	γ-Fe_2O_3	8.3363	8.3363	8.3363	21.2
A250	γ-Fe_2O_3	8.2680	8.2680	8.2680	24.5
A500	γ-Fe_2O_3, α -Fe_2O_3	8.2331	8.2331	8.2331	25.8
A850	α -Fe_2O_3	4.9876	4.9876	13.6114	42.3
B	γ-Fe_2O_3	8.5220	8.5220	8.5220	2.1
B250	γ-Fe_2O_3	8.2915	8.2915	8.2915	8.6
B500	γ-Fe_2O_3	8.2341	8.2341	8.2341	35.4
B850	α -Fe_2O_3	4.9584	4.9584	13.5070	58.5

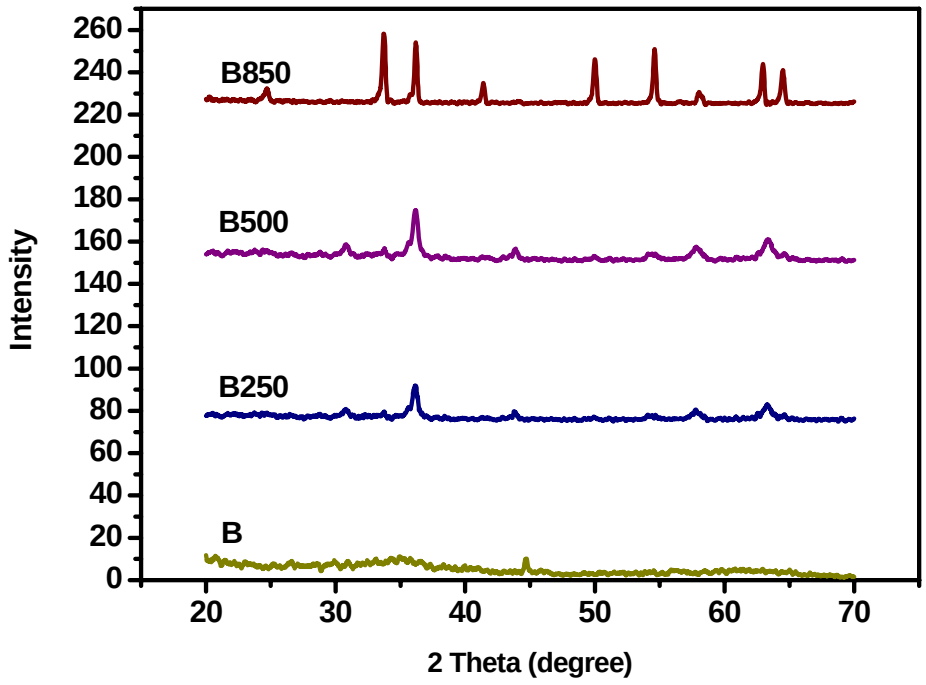

Figure 3. XRD patterns of sample B, B250, B500 and B850.

3.3 SEM and TEM Analysis

The morphology of iron oxide samples are shown in figures 4(a) to 4(e) as obtained from SEM and TEM.

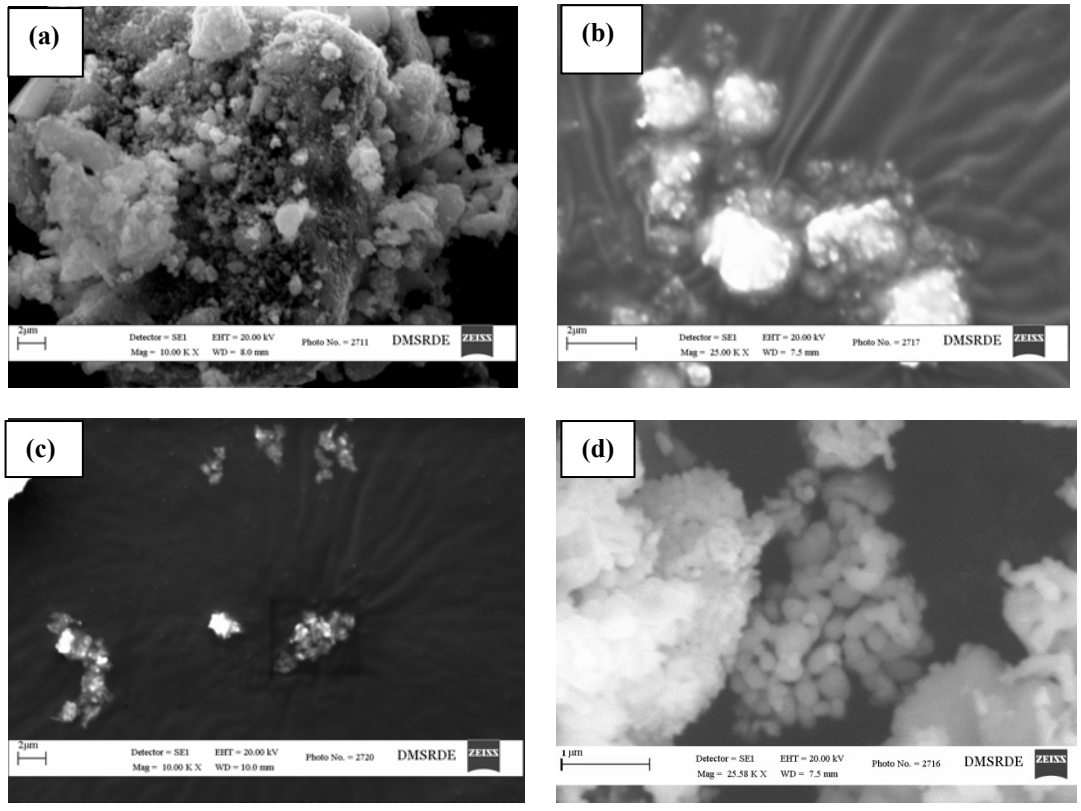

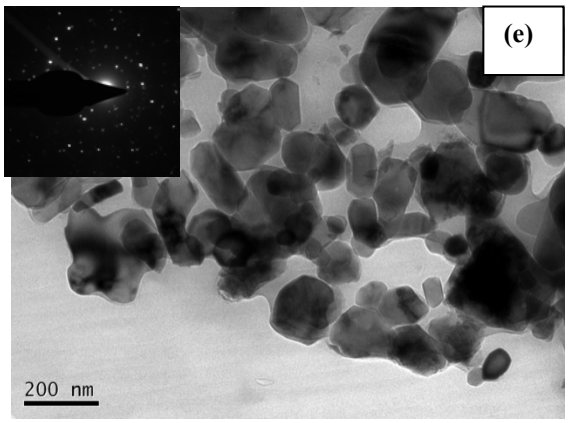

Figure 4. SEM micrograph of (a) Sample A, (b) Sample A500, (c) Sample A850, (d) Sample B850 and (e) TEM image of Sample B850.

Sample A is irregular, bulkier and agglomerated. Increasing calcination temperature resulted in particles becoming more fine and uniform as observed from figures 4(b) and 4(c)]. Fig 4(d) and 4(e) show the SEM and TEM micrographs, respectively for sample B850. The particles are well dispersed, very fine and hexagonal single crystals with particle size of ~70-100 nm. The selected area electron diffraction (SAED) pattern of the sample shows clear diffraction spots (inset in figure 4e), which indicates the high crystallinity of hematite nanoparticles (Kim *et al.*, 2010).The average crystallite size of B850 was found 58.5 nm from XRD, which is in good agreement with TEM result. The well dispersed and single crystal particles of nano hematite (B850) are because of growth of bigger crystals with less strain among the particles at the time of synthesis. Surface energy and lattice strain play important role for synthesis of nanoparticles and growing of crystal (Yen *et al.*, 2002).

3.4 Rheological behavior

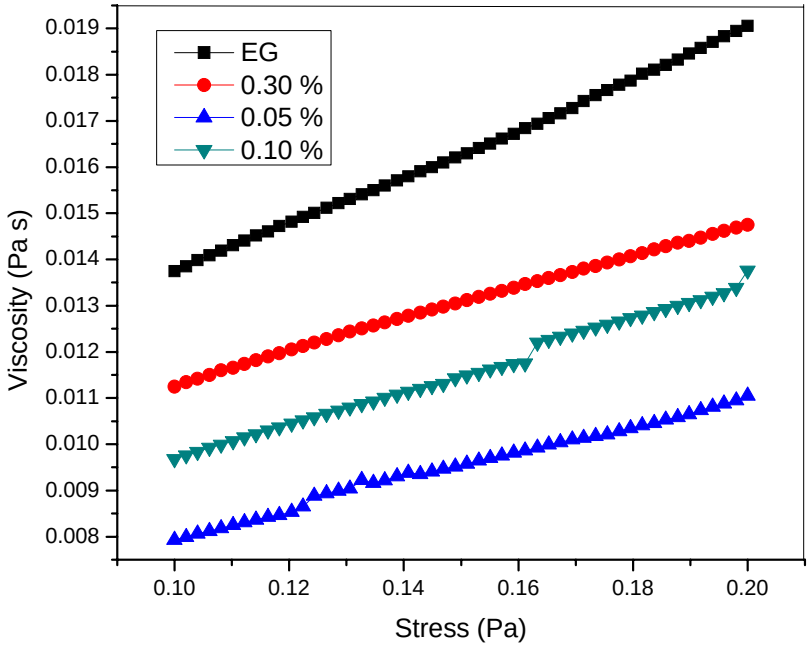

Figure 5. Variation of viscosity with stress for α-Fe_2o_3 nanoparticles in ethylene glycol (EG) for different concentrations.

The rheological tests were carried out for B850 ferrofluids with stress varying from 0.2 to 0.1 Pa to avoid the effects due to inertia yielding shear rate of 1 to 50 s^{-1} and secondary flows due to the electro rheological ferrofluids (ERF) having very low concentration. All the prepared ferrofluids show linearity in nature, which indicate Newtonian behavior of the ferrofluids (Espı´n *et al.*, 2004).

4. Conclusions

The following conclusions are drawn from the above study:

1. Nano crystalline α- and γ-iron oxides were synthesized by emulsion assisted precipitation-calcination method.
2. The as synthesized precursor samples were calcined at 250, 500 and 850 °C. The inverse spinel maghemite phase transformed completely into rhombohedral hematite at a calcination temperature of 850 °C. With increase in calcination temperature, average crystallite size increased and lattice parameters '*a*' and '*b*' decreased. The lattice parameter while '*c*' decreased upto a calcination temperature of 500 ^{o}C followed by increase for samples calcined at 850^{o}C. Also for lower initial iron concentration, pure maghemite phase was formed at a calcination temperature of 500°C.
3. Scanning electron micrographs clearly showed that with the increase in calcination temperature, agglomeration decreased. A typical TEM image confirmed the well dispersed particles of hematite obtained when lower initial concentration (0.1M) of iron salt was used during synthesis.
4. From rheological study, it was observed that the prepared α-Fe_2O_3 based ferrofluids show Newtonian behavior.

Acknowledgements

The authors are thankful to Dr. A. Subhananda Rao, Distinguished Scientist and Director, HEMRL, Pune, for his kind permission to publish this paper.

References

Baruwati B., Reddy K., Madhusudan M., and Sunkara V., 2006. Synthesis of nanostructured hydroxides and oxides of iron: Control over morphology and physical properties. *J. Am. Ceram. Soc.* Vol. 89, No.8, pp. 2602-2605.

Bate G., 1975. Magnetic Oxides, Part II, Craik, D. J., Ed.; John Wiley: New York, p 703.

Cao H., Wang G., Zhang L. Liang Yu., Zhang S., and Zhang X., 2006. Shape and magnetic properties of single-crystalline hematite (α-Fe_2O_3) nanocrystals, *Chem. Phys. Chem.* Vol. 7, No. 9, pp.1897-1901.

Cao M.H., Liu T.F., Gao S., Sun G.B., Wu, X. L., Hu C.W., and Wang Z.L., 2005. Single-crystal dendritic ,micro-pines of magnetic α-Fe_2O_3: Large-scale synthesis, formation mechanism, and properties. *Angew. Chem. Int. Edn.* Vol. 44, No. 27, 4197-4201.

Chen J., Xu L., Li W.Y., and Gou X.L., 2005. α-Fe_2O_3 nanotubes in gas sensor and lithium-ion battery applications. *Adv. Mater.* Vol.17, No. 5, pp. 582-585.

Cornell R. M., and Schwertmann U.,1996. The Iron Oxides; Structure, Properties, Reactions, Occurrence and Uses. VCH Weinheim, New York.

Daou T.J., Greneche J-M., Lee S-J., Lee S., Lefevre C., Sylvie B-C., and Pourroy G., 2010. Spin canting of maghemite studied by NMR and In-Field Mossbauer spectrometry. *J. Phys. Chem.C* Vol. 114, No. 19, pp. 8794-8799.

Dar M.A., Kulkarni S.K., Ansari A., Ansari, S.G., and Hyung-Shik S., 2005. Preparation and characterization of α-FeOOH and α-Fe_2O_3 by sol–gel method. *J. Mater. Sc.,* Vol. 40, No.11, pp. 3031-3034.

Deb P., and Basumallick A., 2004. Phase evolution of iron oxide nanoparticles prepared by heat treatment of a non-aqueous precursor. *Institute of Eng (India)-Mater. Miner.* Vol. 85 (April), pp.1-6.

Dong W.T., and Zhu C.S., 2002. Use of ethylene oxide in the sol–gel synthesis of α-Fe_2O_3 nanoparticles from Fe(III) salts. *J. Mater. Chem.* Vol.12, No.(6), pp.1676.

Espı´n M.J., Delgado A.V., Martin J.E. (2004). Effects of electric fields and volume fraction on the rheology of hematite/silicone oil suspensions. *Rheol Acta*. Vol. 44, pp. 71–79

de Faria D.L.A., Silva, S.V., and de Oliveria M.T., 1997. Raman microspectroscopy of some iron oxides and oxyhydroxides. *J. Raman Spectrosc.* Vol. 28, No. 11, pp. 873–878.

Figuerola A., Corato R.D., Manna L., and Pellegrino T., 2010. From iron oxide nanoparticles towards advanced iron-based inorganic materials designed for biomedical applications. *Pharmacological Research* Vol. 62, No. 2, pp. 126-143.

Fischer S.H., and Grubelich M.C.,1998. Proceedings of the 24th International Pyrotechnics Seminar, IIT Research Institute Chicago, Theoretical energy release of thermites, intermetallics and combustible metals, July 27–31, pp. 231-286.

Giria S., Samantab, S., Majic S., Gangulic S., and Bhaumik A., 2005. Magnetic properties of α-Fe_2O_3 nanoparticle synthesized by a new hydrothermal method. *J. Magnetism and Magnetic Materials* Vol. 285, No. 1-2, pp. 296-302.

Glotch T.D., and Rossman G.R., 2009. Mid-infrared reflectance spectra and optical constants of six iron oxide/oxyhydroxide phases. *Icarus* Vol. 204, No. 2, pp. 663- 671.

Gupta A.K., and Gupta M., 2005. Synthesis and surface engineering of iron oxide nanoparticles for biomedical applications. *Biomaterials* Vol. 26, No. 18, pp. 3995-4021.

Gurmen S., and Ebin B., 2010. Production and characterization of the nanostructured hollow iron oxide spheres and nanoparticles by aerosol route. *Journal of Alloys and Compounds* Vol. 492, No. 1-2, pp. 585-589.

Huo L., Li W., Lu L., Cui H., Xi S., Wang J., Zhao B., Shen Y., and Lu Z., 2000. Preparation, structure, and properties of three-dimensional ordered α-Fe_2O_3 nanoparticulate film. *Chem. Mater.* Vol. 12, No. 3, pp. 790.

Jia B., Gao L., and Sun J., 2007. Synthesis of single crystalline hematite polyhedral nanorods via a facile hydrothermal process *J. Am. Ceram. Soc.* Vol. 90, No. 4, pp. 1315–1318.

Jia C.J., Sun L.D., Yan Z.G., You L.P., Luo F., Han X.D., Pang Y.C., Zhang Z., and Yan C., 2005. Electrophilic activation and cycloisomerization of enynes: A new route to functional cyclopropanes. *Angew. Chem. Int. Edn.* 44(28), 4328-4333.

Kim Il T., Nunnery G. A., Jacob K., Schwartz J., Liu X., and Tannenbaum R., 2010. Synthesis, characterization, and alignment of magnetic carbon nanotubes tethered with maghemite nanoparticles. *J. Phys. Chem. C* Vol.114, No.15, pp. 6944–6951.

Kodama R.H., Makholoufand S.A., and Berkowitz A.E., 1997. Finite size effects in antiferromagnetic NiO nanoparticles. *Phys. Rev. Lett.* Vol. 79, No. 7, pp. 1393-1396.

Kumfer B.M., Shinoda K., Jeyadevan B., and Kennedy I.M., 2010. Gas-phase flame synthesis and properties of magnetic iron oxide nanoparticles with reduced oxidation state. *Journal of Aerosol Science* Vol. 41, No. 3, pp. 257-265.

Laurent S., Forge D., Port M., Roch A., Robic C., Elst L. V., and Muller R.N., 2008. Magnetic iron oxide nanoparticles: Synthesis, stabilization, vectorization, physicochemical characterizations, and biological applications. *Chem. Rev.* Vol. 108, No.6, pp. 2064-2110.

Leoni M., Maggio R.D., Polizzi S., and Scardi P., 2004. X-ray diffraction methodology for the microstructural analysis of nanocrystalline powders: Application to cerium oxide. *J. Am. Ceram. Soc.* Vol. 87, No.6, pp. 1133-1140.

Maensiri S., Masingboon C., Laokul P., Jareonboon W., Promarak V., Anderson P.L., and Seraphin S., 2007. Egg white synthesis and photoluminescence of platelike clusters of CeO_2 nanoparticles. *Crystal Growth and Design* Vol.7, No.5, pp. 950-955.

Massart R.,1981.Preparation of aqueous magnetic liquids in alkaline and acidic media. *IEEE Trans. Magn.* Vol. 17, No. 2, pp. 1247-1248.

Millan A., Palacio F., Falqui A., Snoeck E., Serin V., Bhattacharjee A., Ksenofontov V., Gu¨tlich P., and Gilbert I., 2007. Maghemite polymer nanocomposites with modulated magnetic properties. *Acta Mater.* Vol. 55, No. 6, pp. 2201–2209.

Music S., Czako-nagy I., Salai-obelic I., and Ljubesic N., 1997. Formation of α-Fe_2O_3 particles in aqueous medium and their properties. *Mater. Lett.* Vol. 32, No. 5-6, pp. 301-305.

Music S., Krehula S., Popovi´c S., and Skoko Z., 2003. Some factors influencing forced hydrolysis of $FeCl_3$ solutions. *Mater. Lett.* Vol. 57, No. 5-6, pp. 1096-1102.

Pecharroman C., Gonzales-Carreno T., and Iglesias J.E., 1995. The infrared dielectric properties of maghemite, γ-Fe_2O_3, from reflectance measurement on pressed powders. *Phys. Chem. Miner.* Vol. 22, No. 1, pp. 21–29.

Prakash A., McCormick A.V., and Zachariah M.R., 2004. Aero-Sol−Gel synthesis of nanoporous iron-oxide particles: A potential oxidizer for nanoenergetic materials. *Chem. Mater.* Vol. 16, No. 8, pp. 1466-1471.

Praserthdam P., Mekasuwandumrong O., Phungphadung J., Kanyanucharat, A., 2003. New correlation for the effects of the crystallite size and calcination temperature on the single iron oxide nanocrystallites. *Crystal Growth and Design* Vol. 3, No. 2, pp. 215-219.

Randrianantoandro N., Mercier A.M., Hervieu M., and Greneche J.M., 2001. Direct phase transformation from hematite to maghemite during high energy ball milling. *Mater. Lett.* Vol. 47, No. 3, pp.150-158.

Scardi P., 1999. A new whole powder pattern approach. In X-ray Powder Diffraction Analysis of Real Structure of Materials, International Union of Crystallography Series; Bunge, H.-J., Fiala, J, Snyder, R.L., Eds.; Oxford University Press: Oxford, U.K., p 570.

Tueros M.J., Baum L.A., Borzi R.A., Stewart S.J., Mercader R.C., Marchetti S.G., Bengoa J.F., and Mogni L.V., 2003. Characterization of nanosized maghemite particles prepared by microemulsion using an ionic surfactant. *Hyperfine Interact.* Vol. 14, No. 1-4, pp.103.

Vayssieres L., Sathe C., Butorin S.M., Shuh D.K., Nordgren J., and Guo J-H, 2005. One-dimensional quantum-confinement effect in α-Fe_2O_3 ultrafine nanorod arrays. *Adv. Mater*. Vol. 17, No. 19, pp. 2320-2323

Wang J., and Meng J., 2001. Magnetorheological fluid devices: principles, characteristics and applications in mechanical engineering. *Proc Instn Mech Engrs* Vol.215 (Part L), pp. 165-174.

Wen X.G., Wang S.H., Ding Y., Wang Z.L., and Yang S.H., 2005. Controlled growth of large-area, uniform, vertically aligned arrays of α-Fe_2O_3 nanobelts and nanowires. *J. Phys. Chem.* B Vol. 109, No. 1, pp. 215-220.

White W.B., and Deangelis B.A., 1967. Interpretation of the vibrational spectra of spinels. *Spectrochim. Acta, Part A Molecular Spectroscopy* Vol. 23A, No. 4, pp. 985-995.

Woo K., Lee H.J., Ahn J.P., Park Y.S., 2003. Sol–Gel mediated synthesis of Fe_2O_3 nanorods. *Adv. Mater*. Vol. 15, No. 20, pp. 1761-1764.

Yen F. S., Chen W.C., Yang J.M., and Hong C.T., 2002. Crystallite size variations of nanosized Fe_2O_3 powders during γ- to α-phase transformation. *Nano Letters* Vol. 2, No. 3, pp. 245-252.

Zhao B., Wang Y., Guo, H., Wang J., He Y., Jiao Z., Wu M., 2007. Iron oxide(III) nanoparticles fabricated by electron beam irradiation method. *Materials Science Poland* Vol. 25, No. 4, pp. 1143-1148.

Biographical notes

S.K. Sahoo is a Scientist in High Energy Materials Research Laboratory (DRDO), Pune, India. He is working in the field of nanomaterials (metal oxides: pure and doped) synthesis, characterization and their applications. Presently, he is involved in preparing metastable intermolecular composites (MIC) and their thermite application in pyrotechnics. He is also interested in crystallographic studies of nanostructured materials.

K. Agarwal is working as a Scientist at DMSRDE (DRDO), Kanpur, India. Her field of research includes characterization of micro- and nano-materials by spectroscopic technique such as scanning electron microscope. She is doing her Ph. D. in Physics at DIAT, (deemed University), Pune, India. Presently her area of research includes incorporation of nanomaterials in polymers and studies of various properties.

A. K. Singh obtained his M.Sc. degree from Agra University Agra, India, in the year 1986 and Ph.D. degree from University of Rajasthan, Jaipur, India, in the year 1992. He is working as a Scientist at DIAT, Pune, India. Presently, he is involved in synthesis and characterisation of nanostructures using chemical, physical methods and thin film deposition for sensing applications and other applications. He is also involved in thermal and rheological properties of nanofluids, design and development of instrumentation for measuring thermal properties, piezoelectric sensors / actuators and gas detection. He has been awarded with DRDO Laboratory Scientist of the year award 2005, DIAT Researcher of the Year Award 2008 and is life member of Instrumentation Society of India. He has published about 80 scientific papers in journals and conference proceedings of national and International repute.

B.G. Polke has completed his MSc. degree in Physical Chemistry from Pune University. Pune, India. He has long experience in analysis and characterization of high energy materials. He has also worked in the field of pilot plant studies of energetic materials. He has 10 publications in international and 2 in national journals. He is an active member of High Energy Materials Society of India, Electron Microscopy Society of America and Polymer Society of India.

K.C. Raha obtained his MSc in Physical Chemistry from Calcutta University in 1971. He worked as Research Fellow initially in IACS and then at CGCRI Jadavpur, Kolkata, during 1972-1976. He obtained PhD degree in Solid State Chemistry (Explosive) from Pune University in 1984.He has more than 33 years of research experience in the field of propellant, explosives and pyrotechnics. Presently he is working as Associate Director in HEMRL (DRDO), Pune, India. He has published more than 100 papers and reports in various journals and seminars proceedings.

Received May 2010
Accepted November 2010
Final acceptance in revised form November 2010